
Global Robustness Verification Networks

Weidi Sun

School of Mathematical
Peking University
Haidian Qu 100871, Beijing, China
weidisun@pku.edu.cn

Coauthor

Yuteng Lu
School of Mathematical
Peking University
Haidian Qu 100871, Beijing, China
1701210111@pku.edu.cn

Coauthor

Xiyue Zhang
School of Mathematical
Peking University
Haidian Qu 100871, Beijing, China
zhangxiyue@pku.edu.cn

Coauthor

Zhanxing Zhu
School of Mathematical
Peking University
Haidian Qu 100871, Beijing, China
zhanxing.zhu@pku.edu.cn

Coauthor

Meng Sun
School of Mathematical
Peking University
Haidian Qu 100871, Beijing, China
Center for Quantum Computing, Peng Cheng Laboratory
Shenzhen Shi 518055, China
sunmeng@math.pku.edu.cn

Abstract

The wide deployment of deep neural networks, though achieving great success in many domains, has severe safety and reliability concerns. Existing adversarial attack generation and automatic verification techniques cannot formally verify whether a network is *globally robust*, i.e., the absence or not of adversarial examples in the input space. To address this problem, we develop a global robustness verification framework with three components: 1) a novel rule-based “back-propagation” finding which input region is responsible for the class assignment by logic reasoning; 2) a new network architecture *Sliding Door Network (SDN)* enabling feasible rule-based “back-propagation”; 3) a region-based global robustness verification (RGRV) approach. Moreover, we demonstrate the effectiveness of our approach on both synthetic and real datasets.

1 Introduction

Deep Neural Networks (DNNs) have been applied to a variety of domains and achieved great success. Reliance on DNNs’ decisions makes their behavior reliability of high importance. Recent research has shown that the safety of DNNs is threatened by their susceptibility to human-imperceptible adversarial perturbations [14, 4, 1].

To explore the adversarial robustness of neural networks, two aspects have been considered: *crafting adversarial examples* and *automatic verification*. Given an input sample, adversarial example generation techniques [13, 2, 10, 15, 6] fail to guarantee that no adversarial example exists around

the given input, when they cannot generate adversarial examples for it. The efforts in *automatic verification* mainly focus on the guarantee of local robustness [9, 5, 16, 11, 3], i.e., the robustness of an input’s neighborhood. These verification approaches can provide a rigorous local robustness proof if adversarial examples do not exist in a local region. However, the local robustness only takes a small part of the input space into account, and thus cannot guarantee reliability of the whole network for every possible input.

Some attempts have been made towards the verification and evaluation of *global robustness*, i.e., finding out whether no adversarial example exists in the input space of a network [12, 6]. Though the SMT/SAT-based method in [6] takes global robustness into account, the definition for global robustness in [6] cannot be satisfied by the inputs near the classification boundary. In other words, no network can satisfy this definition. The technique developed in [12] evaluates the local robustness of each sample in a test dataset and treats the expected value of evaluation results as the indicator of “global robustness”. The technique in [12] can be considered as finding expected maximum safe radius over the test dataset. Thus, the selection of the test dataset directly influences the estimation in [12], and the global robustness cannot be formally guaranteed in general. We can easily identify two stumbling blocks on the path of global robustness verification: the *complex activation patterns* and *large input space*. It is computationally prohibited to analyze all possible activation patterns or traverse input space to guarantee global robustness. Thus existing testing and verification techniques are infeasible to handle the global robustness verification for DNNs.

In this paper, we develop a feasible global verification framework with three components: 1) a novel rule-based “back-propagation” which is used for mapping classification rules from output to input to find which input region is responsible for the corresponding class assignment¹, 2) a new network design *Sliding Door Network (SDN)* that enables feasible rule-based “back-propagation”, 3) a region-based global robustness verification (RGRV) approach by finding “adversarial regions”. Particularly, we address the “two stumbling blocks” by two means. Firstly, we design a new activation function *Sliding Door Activation (SDA)*, with which the number of possible activation patterns is dramatically reduced to circumvent the complexity issue. Secondly, instead of treating a single input as the foundation “atom” of global robustness analysis, we cluster the input space into multiple classification regions to address the input space explosion challenge. To the best of our knowledge, this is the first work that can achieve global robustness formally with only slight drop of classification accuracy compared with classic DNNs. We evaluate the effectiveness of our framework on the MNIST [8] dataset. We also design a synthetic case study to show the feasibility of our global verification method.

The rest of this paper is structured as follows. We introduce the rule-based “back-propagation” in Section 2. The network design and the corresponding rule-based back-propagation method are described in Section 3. Section 4 presents the RGRV approach. We evaluate the usefulness of SDN and effectiveness of RGRV in Section 5. Section 6 summarizes our work.

Notations. For the convenience of presentation, each traditional layer $Layer^h$ ($0 < h \leq H$) is treated as two virtual layers: pre-activation and activation layer, denoted by L^h and L'^h , respectively. An example is shown in Figure 1, where the activation layers are L^1, L^2, L^3 and the pre-activation ones are L'^1, L'^2, L'^3 . The i -th neurons in L^h and L'^h are denoted as x_i^h and $x'_i{}^h$, respectively; the weights and the corresponding biases connecting L^{h-1} and L^h are represented as ω_{ij}^h and b_j^h ; the activation function of L'^h is f^h , such as ReLU or softmax.

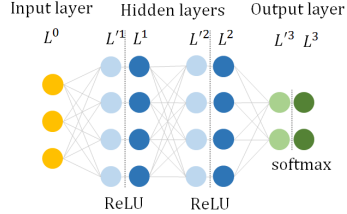


Figure 1: A DNN with two hidden layers and one output layer.

2 Rule-based back-propagation for DNNs

Due to the colossal input space of DNNs, exhausting all possible inputs with traditional testing methods is infeasible. Thus we develop a family of classification rules to divide the input space into several regions. These regions can simplify the global robustness verification significantly. The

¹Note that this “back-propagation” is entirely different from typical use of back-propagation for evaluating the gradient with respect to the weight parameters in DNNs.

classification rules in the input space could be achieved by the proposed rule-based back-propagation, as elaborated below. Before introducing the classification rules in detail, we first present a warm up example.

Example 1. Considering the one-layer network in Figure 2(a), a classification rule in the output space is $(y_0 > y_1)$ which represents a blue region in output space shown as Figure 2(b). The back-propagation we proposed aims for mapping classification rules to the input space. For example, the activation pattern “all neurons are active” means that $(y_0 = y'_0 \wedge y_1 = y'_1 \wedge y'_0 > 0 \wedge y'_1 > 0)$. As $(y_0 = y'_0 \wedge y_1 = y'_1 \wedge y'_0 = x_1 \wedge y'_1 = x_0)$, $(y_0 > y_1)$ is equivalent to $(x_1 > x_0)$ and $(y'_0 > 0 \wedge y'_1 > 0)$ is equivalent to $(x_1 > 0 \wedge x_0 > 0)$. Thus the mapping result of output space $(y_0 > y_1)$ to input space is $(x_0 > 0 \wedge x_1 > 0 \wedge x_1 > x_0)$. If we change the activation pattern to “ y_0 is active and y_1 is inactive”, the equivalent condition of this activation pattern is $(y_0 = y'_0 \wedge y_1 = 0 \wedge y'_0 > 0 \wedge y'_1 < 0)$, because ReLU assigns 0 to y_1 . Thus $(y'_0 > 0 \wedge y'_1 < 0)$ is equivalent to $(x_1 > 0 \wedge x_0 < 0)$; $(y_0 > y_1)$ is equivalent to $(x_1 > 0)$; the mapping result is $(x_0 < 0 \wedge x_1 > 0)$. Obviously, the activation pattern determines the mapping result. The mapping result $(x_0 > 0 \wedge x_1 > 0 \wedge x_1 > x_0)$ represents a blue region in input space shown in Figure 2(c). We name this blue region as classification region, indicating its responsibility to the class assignment.

With the intuition from the warm up example, we now elaborate the rule-based back-propagation layer by layer for deep neural networks.

There are many inequations recorded as $\mathbb{P}_{\gamma\eta}^h$ in $Layer^h$. These inequations make up the disjunctive normal form $\bigvee_{\gamma} \bigwedge_{\eta} \mathbb{P}_{\gamma\eta}^h$ which describes how neural networks classify the inputs. For simplicity, if we select a $\mathbb{P}_{\gamma\eta}^h$ in $Layer^h$ this $\mathbb{P}_{\gamma\eta}^h$ will be denoted as $\mathbb{P}^h = \sum_i c_i x_i^h + b > 0$. We can easily provide

the classification rules in output space. For example, “the output belongs to class k ” is $\bigwedge_{j(j \neq k)} y_k > y_j$

where y_j s ($0 \leq j < m$) are the output values and m is the number of classes for output. To obtain the classification rules in input space, we take a typical DNN² as an example and propose a back-propagating function. During the back-propagation from $Layer^h$ to $Layer^{h-1}$, the \mathbb{P}^h s should be substituted and the \wedge s and \vee s should be retained to $Layer^{h-1}$, thus we apply our function to each \mathbb{P}^h instead of the conjunctive normal form. The recursive call of this function can back-propagate the classification rules layer by layer to the input space of the network. Since the output layer and the hidden layers should be treated in different ways, we divide the function into two parts: the output and hidden layer part.

The comparison rules like $y_k > y_j$ can be directly mapped to the corresponding pre-activation layer based on the order-preserving activation function, e.g., softmax, of the output layer. We replace every variable y_j in inequations with the corresponding polynomial $\sum_i \omega_{ij}^H x_i^{H-1} + b_j^H$ to obtain the classification rule in $Layer^{H-1}$. Thus the output layer part is the function

$$MAP-OUT(y_k > y_j) = \sum_i \omega_{ik}^H x_i^{H-1} + b_k^H > \sum_i \omega_{ij}^H x_i^{H-1} + b_j^H \quad (1)$$

and the mapping result of $\bigwedge_{j(j \neq k)} y_k > y_j$ is $\bigwedge_{j(j \neq k)} MAP-OUT(y_k > y_j)$, i.e., the classification rules in $Layer^{H-1}$.

The hidden layer part is a function $MAP-HIDDEN$. Since each linear inequation in L^h can be simplified into the form $\sum_i c_i x_i^h + b > 0$, we select an inequation $\mathbb{P}^h = \sum_i c_i x_i^h + b > 0$ as the input of $MAP-HIDDEN$ to show how $MAP-HIDDEN$ works. The hidden layers cannot be processed in the same way as output layer because of the activation patterns which determine the mapping result. We denote the set of active neurons' indexes by Θ and use Θ to represent the activation pattern. For

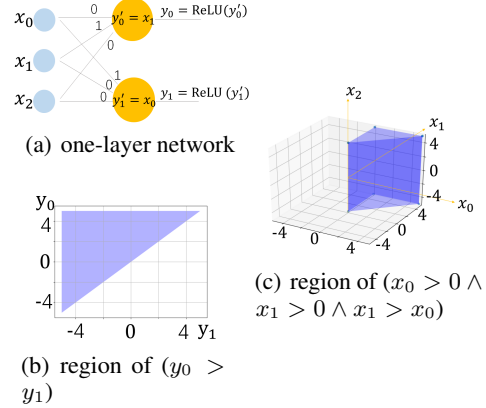


Figure 2: The one-layer network and regions of classification rules.

²The activation functions in hidden layers and output layer of this DNN are ReLU and softmax, respectively.

simplicity, we record the mapping result of \mathbb{P}^h under Θ^h as $MAP-FIX(\Theta^h, \mathbb{P}^h)$ where Θ^h is the activation pattern of $Layer^h$. $MAP-FIX(\Theta^h, \mathbb{P}^h)$ is the conjunction of some classification rules in $Layer^{h-1}$.

The function $MAP-HIDDEN$ is shown as follows where Δ^h denotes all activation patterns of $Layer^h$:

$$MAP-HIDDEN(\Delta^h, \mathbb{P}^h) = \bigvee_{\Theta^h \in \Delta^h} MAP-FIX(\Theta^h, \mathbb{P}^h) \quad (2)$$

The mapping result of $MAP-HIDDEN$ is the disjunction of all the classification rules in $Layer^{h-1}$. As each neuron has two activation states, there are 2^{m^h} activation patterns in Δ^h where m^h is the number of neurons in $Layer^h$. The time cost of whole back-propagation is $O(\prod_h 2^{m^h}) = O(2^{\sum_h m^h})$. Such immense time cost makes the above mapping NP-hard and infeasible.

3 Sliding Door Network for Feasible Back-propagation

To handle the complexity issue, we present a novel network design, SDN, and the corresponding rule-based back-propagation method M_{SDN} . SDN reduces the size of Δ by grouping the neurons in each layer to overcome the infeasibility problem in back-propagating classification rules for DNNs.

3.1 Sliding Door Network

Compared with typical DNNs, SDN has two different components: a novel activation function SDA and the loss function design for supporting SDA.

Sliding Door Activation. SDA takes a pre-activation layer into account and divides neurons into several groups evenly. For example, the layer L^h in Figure 3 with 10 neurons is divided into 5 groups which are represented as $G_j^h = \{x_i^h | 2j \leq i < 2j + 2\}$ ($0 \leq j < 5$). These groups are classified by SDA into three categories: *active group* with all positive neurons (e.g., G_1^h and G_4^h in Figure 3), *inactive group* in which all neurons are negative (e.g., G_3^h in Figure 3), and *trivial groups* with mixing of both positive and negative neurons (i.e., G_0^h and G_2^h in Figure 3).

In order to reduce the complexity, we select the first active (inactive) group as *active (inactive) door* for each pre-activation layer. For example in Figure 3, G_1^h and G_3^h are active door and inactive door respectively. Based on the assigned doors, we define SDA as:

$$x_i^h = SDA(x_i^h) = \begin{cases} 0 & \text{if } x_i^h \text{ belongs to inactive door;} \\ \alpha x_i^h & \text{if } x_i^h \text{ belongs to active door;} \\ x_i^h & \text{otherwise.} \end{cases} \quad (3)$$

To increase the network expressiveness, SDA strengthens the active door by α and assigns 0 to inactive door's neurons. Other groups are sent to the corresponding activation layer directly. During the training, for each pre-activation layer, the position of the two doors might change instantly up to the states of the groups, behaving like a sliding door, thus the name of our activation function. Figure 4 shows the entire network architecture, replacing the ReLU in classic DNNs with the proposed SDA for each layer.

Loss function design. If a pre-activation layer cannot provide *active* or *inactive* door, the expressiveness of SDN will be weakened. To avoid this issue, we design regularization term to penalize the absence of either of the two doors. If the active (inactive) door does not appear in L^h , we will find the group G_α^h (G_β^h) in L^h with most

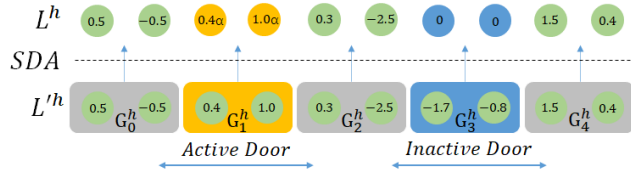


Figure 3: Sliding Door Activation. G_1^h and G_3^h are active door and inactive door respectively and other activation results are the copy of other groups.

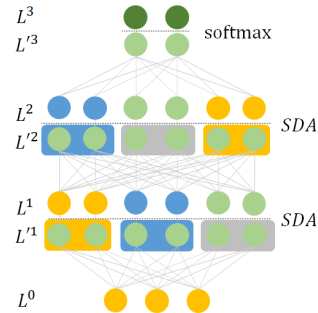


Figure 4: Architecture of SDN

active (inactive) neurons, and adjust the weights to make the negative (positive) neurons in G_α^h (G_β^h) tend to be positive (negative) so as to create active (inactive) groups. Thus, besides the typical data fitting loss, we add a regularization term to encourage the emergence of such groups, defined as:

$$L(W, b) = \sum_{i=1}^n (y_i - \hat{y}_i)^2 + \lambda \sum_h \left(\sum_{x_i^h \in G_\alpha^h, x_i^h < 0} (-x_i^h) + \sum_{x_i^h \in G_\beta^h, x_i^h > 0} x_i^h \right) \quad (4)$$

where $\{W, b\}$ denotes all the weights and biases to be trained, and λ is the user-given penalty parameter.

3.2 Rule-based Back-propagation for SDN

As *MAP-OUT* can be reused for the back-propagation of SDN's output layer, we focus on back-propagation between hidden layers in this section. The constructing process of *MAP-HIDDEN* for SDN is as follows.

We denote the set of neurons in the active door of layer L^h as Θ_A^h , the set of neurons in the inactive door as Θ_I^h , and other neurons are in Θ_T^h . Considering the condition that a rule in L^h is $\mathbb{P}^h = \sum_i c_i x_i^h + b > 0$, and the activation pattern Θ^h is fixed where $\Theta^h = \{\Theta_A^h, \Theta_I^h, \Theta_T^h\}$, we record the mapping result of \mathbb{P}^h under Θ^h as *MAP-FIX*(Θ^h, \mathbb{P}^h) with three components:

1) *SDNInherit*.

$$SDNInherit = \sum_{i \in \Theta_A^h} \alpha c_i \left(\sum_t \omega_{ti}^h x_t^{h-1} + b_i^h \right) + \sum_{i \in \Theta_T^h} c_i \left(\sum_t \omega_{ti}^h x_t^{h-1} + b_i^h \right) + b > 0, \quad (5)$$

where we replace the neurons in \mathbb{P}^h belonging to Θ_A^h with the corresponding polynomial, i.e., $\sum_t \omega_{ti}^h x_t^{h-1} + b_i^h$ multiplied by α due to SDA activation, the neurons in Θ_T^h with the corresponding polynomial meanwhile remove the neurons in Θ_I^h to obtain *SDNInherit*.

2) *SDNActiveCon*.

$$SDNActiveCon = \bigwedge_{i \in \Theta_A^h} \left(\sum_t \omega_{ti}^h x_t^{h-1} + b_i^{h-1} > 0 \right) \quad (6)$$

It describes the rules that “all the corresponding pre-activation neurons of Θ_A^h are greater than 0” and we replace these pre-activation neurons with corresponding polynomial.

3) *SDNInactiveCon*.

$$SDNInactiveCon = \bigwedge_{i \in \Theta_I^h} \left(\sum_t -\omega_{ti}^h x_t^{h-1} - b_i^h > 0 \right) \quad (7)$$

It describes the rules that “all the corresponding pre-activation neurons in Θ_I^h are less than 0” and we replace these pre-activation neurons with corresponding polynomial. The function *MAP-FIX* is shown as follows:

$$MAP-FIX(\Theta^h, \mathbb{P}^h) = SDNInherit \wedge SDNActiveCon \wedge SDNInactiveCon \quad (8)$$

Taking all the activation patterns into account, we can obtain the function *MAP-HIDDEN*.

$$MAP-HIDDEN(\Delta^h, \mathbb{P}^h) = \bigvee_{\Theta^h \in \Delta^h} MAP-FIX(\Theta^h, \mathbb{P}^h) \quad (9)$$

The combination of *MAP-OUT* and *MAP-HIDDEN* is the complete back-propagating function M_{SDN} :

$$M_{SDN}(\Delta^h, \mathbb{P}^h) = \begin{cases} MAP-OUT(\mathbb{P}^h) & h = H \\ MAP-HIDDEN(\Delta^h, \mathbb{P}^h) & h < H \end{cases} \quad (10)$$

Thus the mapping result of all the rules $\bigvee_\gamma \bigwedge_\eta \mathbb{P}_{\gamma\eta}^h$ in *Layer*^h is $\bigvee_\gamma \bigwedge_\eta M_{SDN}(\Delta^h, \mathbb{P}_{\gamma\eta}^h)$ which is the collection of rules for *Layer*_{h-1}. Each $|\Delta^h|$ equals to $m_h(m_h - 1) + 2m_h + 1$ where m_h is the number of groups in L^h . The SDN has $O(\prod_i m_i^2)$ activation patterns which is greatly less than the

number of DNN's activation patterns $O(2^{\sum_h m^h})$ and its rule-based back-propagation becomes more feasible.

M_{SDN} maps the *explicit rules*, but ignores the *implicit rules*. *Implicit rules* are the constraints from *trivial groups* guaranteeing that compared with other active (inactive) groups in $Layer^h$ the active (inactive) door G_i^h has the minimal i . For example in Figure 3, the *implicit rules* are:

$$\exists_{x'_i \in G_0^h} x'_i < 0 \wedge \exists_{x'_i \in G_1^h} x'_i > 0 \wedge \exists_{x'_i \in G_2^h} x'_i > 0$$

The combination of *explicit rules* and *implicit rules* can be organized into the form $\forall_\gamma \wedge_\eta \mathbb{P}_{\gamma\eta}^h$. Each $\wedge_\eta \mathbb{P}_{\gamma\eta}^h$ represents a classification region like the blue region in Figure 2(c). Selecting a $\mathbb{P}^h = \sum_i c_i x_i^h + b > 0$ in $\wedge_\eta \mathbb{P}_{\gamma\eta}^h$, a boundary of $\wedge_\eta \mathbb{P}_{\gamma\eta}^h$'s classification region is $\sum_i c_i x_i^h + b = 0$. We will show that *explicit rules* is sufficient for global verification in Theorem 1.

4 Region-based Global Robustness Analysis

In this section, we define and address the global robustness verification problem by a region-based global robustness analysis (RGRA) approach. Firstly, we provide the definition for global robustness:

Definition 1 (Global robustness). *Given a network N , if there is no adversarial example in its input space, N is a globally robust network.*

An adversarial example exists in two types of regions: 1) the region which is isolated, 2) the region which is connected to the correctly classified region. Taking Figure 5 as an example, it shows a binary classification task where the black dashed line is oracle decision boundary of class C_1 and C_2 and the orange solid line is the decision boundary determined by network. R_1 and R_2 are adversarial regions. R_1 is the *small-size isolated connected component* and R_2 is the *protruding region* which is connected to the correctly classified region. The adversarial examples belonging to C_1 but classified as C_2 tend to exist in R_1 and R_2 . Before presenting the definitions of *protruding region* and *small-size isolated connected components*, we first present a formal definition of the input space classification graph.

Definition 2 (Classification graph). *Given a result of backward-mapping in the form of $\forall_\gamma \wedge_\eta \mathbb{P}_{\gamma\eta}^h$, we can build a classification graph as a tuple (V, E) where*

- $V = \{v_i \mid v_i \text{ is the } \wedge_\eta \mathbb{P}_{\gamma\eta}^h \text{ in } \forall_\gamma \wedge_\eta \mathbb{P}_{\gamma\eta}^h\}$. In other words, each classification region can be defined as a vertex v_i .
- $E = \{(v_i, v_j) \mid v_i \text{ and } v_j \text{ are adjacent vertexes}\}$. Given two vertexes v_i and v_j , the corresponding classification regions in the input space are S_i and S_j . Two vertexes are adjacent iff their classification regions are adjacent in high-dimensional space, and formally,

$$\exists_x \exists_{\varepsilon > 0} \{[\forall_{x' \in I} (x' \in S_i \vee x' \in S_j)] \wedge (I \cap S_i \neq \emptyset) \wedge (I \cap S_j \neq \emptyset)\} \quad (11)$$

where $I = \{x' \mid \|x' - x\|_\infty < \varepsilon\}$.

Definition 3 (Limiting ball). *Given a set of vertexes V' , the stitching of their regions is S whose center of gravity is o . The limiting ball B of V' can be defined as a ball whose center is o and radius $d = \max\{dis \mid dis = \|x - o\|_\infty, x \in S\}$.*

With the description of classification graph and limiting ball, we now provide the formal definition of two types of regions in which adversarial example exist.

Definition 4 (Small-size isolated connected component). *Given a connected component S in classification graph and a \mathcal{R} ($\mathcal{R} > 0$), let B be S 's vertexes' limiting ball. If B 's radius is smaller than \mathcal{R} , S is a small-size isolated connected component.*

Definition 5 (Protruding regions). *Given a vertex v and a r ($r > 0$), let B be $\{v\}$'s limiting ball. The classification region of v is S . All points with same class as S in B constitute a set $Cl(S)$. The volume of $Cl(S)$ and B are recorded as $vol(Cl(S))$ and $vol(B)$ respectively. If S is not a small-size isolated connected component and $vol(Cl(S)) < r \times vol(B)$, S is a protruding region.*

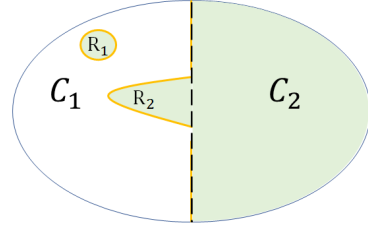


Figure 5: Small-size isolated connected component and protruding region. R_1 and R_2 are the adversarial regions.

The first step of finding the ‘‘adversarial regions’’ is to construct the adjacency relationship between vertexes, i.e., building E in classification graph. The construction can be split into two phases: 1) traverse the vertexes v_i in *classification graph*, and treat v_j ($j \in \{t|t > i\}$) as the potential adjacent vertexes; 2) find the common boundary shared by v_i and v_j if they are adjacent, and provide the proof that they are not adjacent otherwise. Intuitively, a common boundary between v_i and v_j means that they stick together on the boundary, formally defined as follows.

Definition 6 (Common boundary). *Given two vertexes v_i and v_j in the classification graph, the corresponding classification regions are S_i and S_j . A boundary $\mathbb{F} (\sum c_i x_i^0 + b = 0)$ which belongs to v_i and v_j is defined as a common boundary iff*

$$\exists x_0 \exists \varepsilon_0 > 0 [\forall_{\mathbb{H}' \neq \mathbb{H}} I \cap \mathbb{H}' = \emptyset \wedge \forall_{x \in I} (x \in S_i \vee x \in S_j) \wedge I \cap S_i \neq \emptyset \wedge I \cap S_j \neq \emptyset] \quad (12)$$

where $\mathbb{H} = \{x | \sum c_i x_i^0 + b = 0\}$ is the set of points on \mathbb{F} , \mathbb{H}' is the set of points on other boundaries \mathbb{F}' of v_i and v_j , and $I = \{x | \|x - x_0\|_\infty < \varepsilon_0\}$.

As the *classification graph* is an undirected graph, the first phase only explores the edge (v_i, v_j) ($j > i$) to find the potential adjacent vertex v_j . And the following Theorem 1 implies that by traversing the *explicit rules* of v_i , we can find out all the v_j ($j \in \{t|t > i\}$) which share a common boundary with v_i , i.e., all the adjacent vertexes.

Theorem 1. *Given v_i and v_j ($j > i$), there is a common boundary belonging to the explicit rules of v_i shared by them iff v_i and v_j are adjacent.*

Proof: see appendix.

Finally, the global robust verification can be achieved by the following steps:

1. Build classification graph. We can obtain the vertexes from the back-propagation result. Each vertex has some boundaries. For each boundary \mathbb{F} of v_i , we select some points on it randomly and sample in the tiny neighborhood of these points. By feeding the samples into SDN, we can find out their activation patterns. For example, a sample’s activation pattern represents v_j , as this sample is in the tiny neighborhood of points on \mathbb{F} , \mathbb{F} belongs to v_j . Thus v_i and v_j shares the boundary \mathbb{F} and we add edge (v_i, v_j) to the edge set E .
2. Find the limiting ball of classification regions and connected components. For a classification region S , we can obtain the rough upper and lower bound of each dimension. Taking the inequation $\sum c_i x_i^0 + b > 0$ as an example, if $c_1 > 0$ and $-2 \leq x_i \leq 2$, the lower bound of x_1^0 is $x_1^0 > -((\sum_{i(i \neq 1 \wedge c_i > 0)} 2c_i + \sum_{i(i \neq 1 \wedge c_i < 0)} -2c_i) + b)/c_1$. All these bounds form a ‘‘box’’ including S . We take samples u_t ($0 \leq t < n$) in this ‘‘box’’ and select the samples in S . $o = \sum_t u_t/n$ is the estimated center. Denote $d(u_t, o)$ as the distance between u_t and o , the estimated radius is $\max_t(d(u_t, o))$. Moreover, we can calculate the volume of the ‘‘box’’ $vol(box)$, if there are m samples in S , $vol(s) = \frac{m}{n} vol(box)$. If a connected component consists classification regions S_k s, the estimated center is $o = \frac{\sum_k o_k vol(S_k)}{\sum_k vol(S_k)}$ and $\max_{t,k}(d(u_{kt}, o))$ is the estimating radius where u_{kt} s are the samples in S_k .
3. Find small-size isolated connected components and protruding regions. Given a connected component, by comparing the radius of limiting ball with the \mathcal{R} given by user, we can find out whether a connected component is a small-size isolated connected component. For a classification region belonging to class C , we take n samples in the limiting ball. If m of them belong to C , calculate n/m and compare it with the user given r . Then we can find out whether this region is a protruding region.

5 Experiments

The evaluation of our work concentrates on three aspects: 1) the utility of SDN on classification tasks, 2) generating adversarial examples, 3) the feasibility of global verification. In the first part, we evaluate our method on *MNIST* database with typical DNNs as baseline. In the second part, we show the adversarial examples generated from adversarial regions. In the third part, we design a synthetic case study to show the effectiveness of RGRV.

5.1 Utility on classification task

Due to the reduction of activation patterns, the expressive ability of SDN is slightly inferior to typical DNNs with the same architecture. We empirically show the drop of classification accuracy is acceptable based on two groups of case studies. The first group is the comparison of typical DNNs and SDNs on *MNIST* dataset. The details of SDNs are shown as follows.

Table 1: Classification results on MNIST where sat-rate is the frequency of layers which can provide both active door and inactive door in evaluation

MNIST		(16,12)	(24,18)	(32,24)	(40,30)
SDN	accuracy(%)	95.08	95.24	95.32	95.45
	sat-rate(%)	81.64	85.25	93.49	96.37
DNN	accuracy(%)	97.80	98.12	98.21	98.28

1) Each SDN has two hidden layers $Layer^1$ and $Layer^2$; 2) These SDNs have 16, 24, 32, 40 groups in $Layer^1$, respectively and 12, 18, 24, 30 groups in $Layer^2$, respectively. We name these SDNs as (16,12), (24,18), (32,24), and (40,30) based on their architecture features; 3) Each group in $Layer^1$ has four neurons, and each group in $Layer^2$ has two neurons. 4) The α in these SDNs are set as 2.

Each baseline DNN has two hidden layers. The number neurons in each layer is the same as corresponding SDNs. Cross entropy loss and Adam [7] are used to train all the networks 1500 epochs with batch size 256. The evaluation result is shown in Table 1. Compared with typical DNNs, the accuracy of SDN only drops 2.72, 2.88, 2.89, 2.83 percent respectively. Besides, the accuracy of SDN and the *sat-rate* increase as the numbers of groups in each layer increase.

5.2 Generating adversarial examples

Since our verification method is aimed at global verification, i.e., finding all the adversarial regions in the input space, the generation of attacks is only a by-product. As this generation is not based on local or testing way, it is meaningless to compare its efficiency with state-of-the-art attack generation approaches like [13, 2, 10, 15, 6]. Given parameters $(\mathcal{R}, r) = (0.04, 0.2)$, we show the adversarial examples in SDN (20,20)³ and point out the corresponding adversarial regions.

The digits in the first line of Figure 6 classified as “2” are the adversarial examples of the digits below them classified as “0, 6, 8, 4, 9” respectively. Take 4 as an example, the upper 4 is in “[18,1],[1,15]”, denoting the activation pattern where G_{18}^1 and G_1^2 are active doors, G_1^1 and G_{15}^2 are inactive doors. By inputting “[18,1],[1,15]”, we can find a group of inequations returned by our algorithm, and the conjunction of these inequations represents the corresponding classification region of “[18,1],[1,15]”. The lower 4 classified as 4 is in the activation pattern “[4,10],[1,3]”. The classification region of “[18,1],[1,15]” is the *protruding region* found by our method which is close to “[4,10],[1,3]”’s classification region. Moreover, we have found out that there is only one connected component of class 2 in the input space. Obviously, it is easy to select a large number of adversarial examples in the adversarial regions.



Figure 6: Adversarial examples are in the first line and the samples in second line are classified correctly

5.3 Feasibility of precise global verification

As our work is the first global robustness verification work, there is no baseline method existing for this case study. To draw an exact conclusion whether the results of the proposed method are correct, we train a SDN on a two-dimensional synthetic dataset shown in Figure 7(a). In Figure 7(a), the big blue region at the top-right belongs to the first class and the small blue region at the lower-left which is the “noise” in this dataset belongs to the first class as well. The points in the white region belong to the second class. The classification results of the trained SDN are visually shown in Figure 7(b) where the points in the blue regions belong to the first class and the points in the white region belongs

³(20,20) has 20 groups in $Layer^1$ and $Layer^2$ and each group has three neurons. (20,20) is trained on MNIST images which are resized as 4×4 . All the other settings are same as the SDNs in subsection 5.1.

to the second class. Our method has found the adversarial regions in the orange circles. Obviously, these regions containing adversarial examples are what we do not want. The verification result shows that this SDN is not globally robust.

6 Conclusion

In this paper, we present a novel global verification framework. To the best of our knowledge, this is the first work that provides a complete solution to achieving global robust verification for neural networks. Based on the proposed rule-based back-propagation, we analyze the relationship between activation patterns and classification rules, and thus design a new network SDN. Together with a region-based global robustness analysis approach, the verification can be finished in an acceptable duration, dramatically reducing computational complexity. Our evaluation shows that the SDN can perform comparable with classic DNNs, and favourable, the global verification can be achieved, which is unattainable in the past. We hypothesise that SDN is suitable for safety-critical fields, especially for some classification tasks which are not very complex but eager for strict robustness. Developing verification framework for large-scale networks is our further research direction.

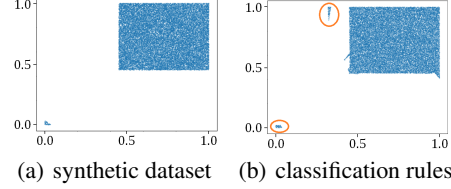


Figure 7: Synthetic dataset and classification rules

7 Appendix

We assign serial numbers to each activation pattern to store the mapping result in a B+ tree for the convenience of global verification:

$$\Theta.number = \sum_h^{n-1} ((g_h * group_num_h + g'_h - 1) \text{ if } (g_h < g'_h) \quad \text{else } (g_h * group_num_h + g'_h)) \\ * \prod_{j=h+1}^n |\Delta'.j| + (g_n * group_num_n + g'_n)$$

where n is the number of layers, h represents $Layer_h$, $g_h(g'_h)$ is the index of $Layer_h$'s active(inactive) door, and $group_num_h$ is the number of groups in L'_h . Two activation patterns Θ_1 and Θ_2 satisfy $\Theta_1.number < \Theta_2.number$ iff

$$(\exists_k \forall_{h(h < k)} \Theta_1.g_h = \Theta_2.g_h \wedge \Theta_1.g'_h = \Theta_2.g'_h) \bigwedge \\ \{\Theta_1.g_k < \Theta_2.g_k \vee (\Theta_1.g_k = \Theta_2.g_k \wedge \Theta_1.g'_k < \Theta_2.g'_k)\}$$

To prove Theorem 1, we need Lemma 1 and Lemma 2.

Lemma 1. *Given two vertexes v_i and $v_j(j > i)$, they are adjacent iff they share a common boundary.*

Proof. Given two adjacent vertexes v_i and $v_j(j > i)$, the corresponding classifications are S_i and S_j . According to the definition of adjacent in Definition 2, there is a x_0 satisfies

$$\exists_{\varepsilon > 0} \{[\forall_{x' \in I} (x' \in S_i \vee x' \in S_j)] \wedge (I \cap S_i \neq \emptyset) \wedge (I \cap S_j \neq \emptyset)\}$$

where $I = \{x' \mid \|x' - x_0\|_\infty < \varepsilon\}$.

There must be a x in I on a boundary F which satisfies $\exists_\varepsilon \forall_{\mathbb{H}_i \neq \mathbb{H}} C \cap \mathbb{H}_i = \emptyset$ where $C = \{x' \mid \|x' - x\|_\infty < \varepsilon_1\}$, \mathbb{H} and \mathbb{H}_i are the point set of boundary F and F_i s. Otherwise we can find a series of points $u_i(i \geq 0)$ and corresponding balls $I_i = \{x \mid \|x - u_i\|_\infty < \sigma_i\}$ satisfying:

- u_i is on the boundary F_i and $\forall_{\varepsilon_i} \mathbb{H}_{i+1} \cap I_i \neq \emptyset$
- $u_{i+1} \in I_i, u_{i+1}$ on $F_{i+1}, I_{i+1} \subseteq I_i$ and $I_{i+1} \cap \mathbb{H}_i = \emptyset$

Since we have only finite number of boundaries, here comes the contradiction. Hence we can find a u_k in I on F which is a boundary of both v_i and v_j and a corresponding I_k satisfies the above condition. As u_k is on the boundary, it satisfies $\forall_{x \in I_k} (x \in S_i \vee x \in S_j) \wedge I_k \cap S_i \neq \emptyset \wedge I_k \cap S_j \neq \emptyset$. Thus u_k satisfies

$$\exists_{\varepsilon_k > 0} [\forall_{\mathbb{H}' \neq \mathbb{H}_k} I_k \cap \mathbb{H}' = \emptyset \wedge \forall_{x \in I_k} (x \in S_i \vee x \in S_j) \wedge I_k \cap S_i \neq \emptyset \wedge I_k \cap S_j \neq \emptyset]$$

and F is a common boundary shared by v_i and v_j .

The sufficient condition is obvious. □

Lemma 2. *Given two adjacent vertexes v_i and $v_j (j > i)$, the shared common boundary of them comes from the explicit rules of v_i .*

Proof. The activation pattern Θ_i and Θ_j of v_i and v_j satisfy $\Theta_i.number = i > \Theta_j.number = j$ thus

$$\begin{aligned} \forall_{t(t < k)} \Theta_i.g_t = \Theta_j.g_t \wedge \Theta_i.g'_t = \Theta_j.g'_t \bigwedge \\ \{\Theta_i.g_k < \Theta_j.g_k \vee (\Theta_i.g_k = \Theta_j.g_k \wedge \Theta_i.g'_k < \Theta_i.g'_k)\} \end{aligned}$$

This indicates the first change of door happens on L'^k . The change of activation pattern leads to the “mutation” of neurons in $L'^t (t > k)$. However the change of neurons in $L'^t (t \leq k)$ is continuous. According to the proof of Lemma 1, we can find a path in D_α which crosses and only crosses the F . Thus When the point on this path approaches the boundary, there is at most one inactive neuron corresponding to F approaches 0 in $L'^t (t \leq k)$. Here we consider where the F comes from:

- F comes from $Layer_t (t > k)$. The change of sign of x'_i will not influence the activation pattern in L'^k which contradicts to “the first change of door happens on L'^k ”
- F comes from $Layer_t (t < k)$. If it changes the activation pattern, it contradicts to “the first change of door happens on L'^k ”. Otherwise, there must be another inactive neuron in L'^k changes the sign at the same time which contradicts to “there is at most one inactive neuron corresponding to F approaches 0 in $L'^t (t \leq k)$ ”
- F comes from *implicit rules* in $Layer_k$. If the activation pattern does not change, here comes the contradiction to “the first change of door happens on L'^k ”. If the activation pattern changes, according to the definition of *implicit rules*, either the index of *active door* g_k or *inactive door* g'_k will become smaller, that is to say, the result is a activation pattern $v_u (u < i)$ instead of v_j . Thus we have a contradiction

We eventually find out that F comes from *explicit rules* of v_i by a process of elimination. □

Based on Lemma 1 and Lemma 2, the correctness of Theorem 1 is obvious.

References

- [1] Battista Biggio, Giorgio Fumera, and Fabio Roli. Security evaluation of pattern classifiers under attack. *CoRR*, abs/1709.00609, 2017.
- [2] Nicholas Carlini and David A. Wagner. Towards evaluating the robustness of neural networks. In *2017 IEEE Symposium on Security and Privacy, SP 2017, San Jose, CA, USA, May 22-26, 2017*, pages 39–57, 2017.
- [3] Timon Gehr, Matthew Mirman, Dana Drachler-Cohen, Petar Tsankov, Swarat Chaudhuri, and Martin T. Vechev. AI2: safety and robustness certification of neural networks with abstract interpretation. In *2018 IEEE Symposium on Security and Privacy, SP 2018, Proceedings, 21-23 May 2018, San Francisco, California, USA*, pages 3–18, 2018.

- [4] Ian J. Goodfellow, Jonathon Shlens, and Christian Szegedy. Explaining and harnessing adversarial examples. In Yoshua Bengio and Yann LeCun, editors, *3rd International Conference on Learning Representations, ICLR 2015, San Diego, CA, USA, May 7-9, 2015, Conference Track Proceedings*, 2015.
- [5] Xiaowei Huang, Marta Kwiatkowska, Sen Wang, and Min Wu. Safety verification of deep neural networks. In *Computer Aided Verification - 29th International Conference, CAV 2017, Heidelberg, Germany, July 24-28, 2017, Proceedings, Part I*, pages 3–29, 2017.
- [6] Guy Katz, Clark W. Barrett, David L. Dill, Kyle Julian, and Mykel J. Kochenderfer. Reluplex: An efficient SMT solver for verifying deep neural networks. In *Computer Aided Verification - 29th International Conference, CAV 2017, Heidelberg, Germany, July 24-28, 2017, Proceedings, Part I*, pages 97–117, 2017.
- [7] Diederik P. Kingma and Jimmy Ba. Adam: A method for stochastic optimization. In *3rd International Conference on Learning Representations, ICLR 2015, San Diego, CA, USA, May 7-9, 2015, Conference Track Proceedings*, 2015.
- [8] Yann LeCun, Corinna Cortes, and Christopher J.C. Burges. The mnist database of handwritten digits. <http://yann.lecun.com/exdb/mnist/>. Accessed January 4, 2020.
- [9] Matthew Mirman, Timon Gehr, and Martin T. Vechev. Differentiable abstract interpretation for provably robust neural networks. In *Proceedings of the 35th International Conference on Machine Learning, ICML 2018, Stockholmsmässan, Stockholm, Sweden, July 10-15, 2018*, pages 3575–3583, 2018.
- [10] Nicolas Papernot, Patrick D. McDaniel, Somesh Jha, Matt Fredrikson, Z. Berkay Celik, and Ananthram Swami. The limitations of deep learning in adversarial settings. In *IEEE European Symposium on Security and Privacy, EuroS&P 2016, Saarbrücken, Germany, March 21-24, 2016*, pages 372–387, 2016.
- [11] Wenjie Ruan, Xiaowei Huang, and Marta Kwiatkowska. Reachability analysis of deep neural networks with provable guarantees. In *Proceedings of the Twenty-Seventh International Joint Conference on Artificial Intelligence, IJCAI 2018, July 13-19, 2018, Stockholm, Sweden*, pages 2651–2659, 2018.
- [12] Wenjie Ruan, Min Wu, Youcheng Sun, Xiaowei Huang, Daniel Kroening, and Marta Kwiatkowska. Global robustness evaluation of deep neural networks with provable guarantees for the hamming distance. In *Proceedings of the Twenty-Eighth International Joint Conference on Artificial Intelligence, IJCAI 2019, Macao, China, August 10-16, 2019*, pages 5944–5952, 2019.
- [13] Fnu Suya, Jianfeng Chi, David Evans, and Yuan Tian. Hybrid batch attacks: Finding black-box adversarial examples with limited queries. *CoRR*, abs/1908.07000, 2019.
- [14] Christian Szegedy, Wojciech Zaremba, Ilya Sutskever, Joan Bruna, Dumitru Erhan, Ian J. Goodfellow, and Rob Fergus. Intriguing properties of neural networks. In *2nd International Conference on Learning Representations, ICLR 2014, Banff, AB, Canada, April 14-16, 2014, Conference Track Proceedings*, 2014.
- [15] Matthew Wicker, Xiaowei Huang, and Marta Kwiatkowska. Feature-guided black-box safety testing of deep neural networks. In *Tools and Algorithms for the Construction and Analysis of Systems - 24th International Conference, TACAS 2018, Held as Part of the European Joint Conferences on Theory and Practice of Software, ETAPS 2018, Thessaloniki, Greece, April 14-20, 2018, Proceedings, Part I*, pages 408–426, 2018.
- [16] Min Wu, Matthew Wicker, Wenjie Ruan, Xiaowei Huang, and Marta Kwiatkowska. A game-based approximate verification of deep neural networks with provable guarantees. *Theor. Comput. Sci.*, 807:298–329, 2020.